Discover Nano

Research

Electrospun nanofibers incorporating lactobionic acid as novel active packaging materials: biological activities and toxicological evaluation

Aline Aniele Vencato[1] · Naiara Jacinta Clerici[1] · André Luiz Mendes Juchem[2] · Flavio Fonseca Veras[1] · Helena Campos Rolla[2] · Adriano Brandelli[1]

Received: 14 May 2024 / Accepted: 16 August 2024
Published online: 31 August 2024

Abstract
In this study, lactobionic acid (LBA) was incorporated into poly(vinyl alcohol) (PVA) and poly(ε-caprolactone) (PCL) by electrospinning. The antimicrobial effects of the nanofibers were tested using the agar diffusion method. Only the PVA formulations showed antimicrobial activity against *Staphylococcus aureus*. The PVA and PCL nanofibers containing LBA showed antioxidant activity ranging from 690.33 to 798.67 µM TEAC when tested by the ABTS method. The characterization of nanofibers was performed by scanning electron microscopy, Fourier transform infrared spectroscopy, thermogravimetric analysis, differential scanning calorimetry, and mechanical analysis. The nanofibers showed a uniform morphology and their average diameters ranged from 295.5 to 2778.2 nm. The LBA addition induced a decrease in the enthalpy of fusion (Δ*H*m) of PVA and PCL nanofibers, while the Young's modulus was reduced from 20 to 10 MPa in PCL and PCL-LBA nanofibers, respectively. No relevant differences were observed between the FTIR spectra of the control nanofibers and the nanofibers containing LBA. All nanofibers presented hemolysis rate below 2%, thus can be considered as non-hemolytic materials. Further toxicological assessment was performed with the selected formulation PVA10 + LBA. The evaluations by mutagenicity assay, cell survival measurement, cell viability analysis and agar diffusion cytotoxicity test indicated that there are no significant toxic effects. Electrospun nanofibers PVA-LBA and PCL-LBA were successfully produced, showing good thermal and mechanical properties and non-toxic effects. Furthermore, the nanofibers showed antimicrobial activity and antioxidant activity. The findings of this study indicate that PVA and PCL electrospun nanofibers incorporating LBA are promising for use in packaging applications.

Keywords Nanofibers · Lactobionic acid · Antibacterial activity · Antioxidant activity · Toxicological evaluation

1 Introduction

Lactobionic acid (LBA) is a natural polyhydroxy acid, composed of a galactose linked to a gluconic acid moiety via an ether-like linkage. LBA is produced by the oxidation of the glucose component of lactose to gluconic acid, showing potential application as natural preservative with antibacterial and antioxidant effects [1, 2]. The antimicrobial

Supplementary Information The online version contains supplementary material available at https://doi.org/10.1186/s11671-024-04084-8.

✉ Adriano Brandelli, abrand@ufrgs.br | [1]Laboratório de Nanobiotecnologia e Microbiologia Aplicada, Instituto de Ciência e Tecnologia de Alimentos, Universidade Federal do Rio Grande do Sul, Av. Bento Gonçalves 9500, Porto Alegre 91501-970, Brazil. [2]NSF International BR, Rua Palermo 257, Viamão 94480-775, Brazil.

activity of LBA has been attributed to the breakdown of structural integrity of the bacterial cell wall and membrane, releasing cellular contents and inhibiting protein synthesis, which causes cell death [3–5].

Lipid oxidation and microbial growth are the main causes of spoilage of a great variety of foods, causing important losses on sensorial and nutritional quality. Active packaging has been studied as an advanced technology to control the growth of spoilage and pathogenic microorganisms and to maintain the quality and safety of food products [2, 4]. However, there is interest to create active packaging materials that are not only antimicrobial, but also antioxidant. In this regard, additional studies are required to develop active packaging materials showing effective antioxidant and antimicrobial properties [5–7].

Currently, packaging materials fabricated from biocompatible and biodegradable polymers attracted more attention due to their safety and environmental appeal. Poly(vinyl alcohol) (PVA) is a hydrophilic synthetic polymer that provides good mechanical properties due to the presence of hydroxyl groups and the formation of hydrogen bonds [8]. Poly(ε-caprolactone) (PCL) is a hydrophobic synthetic polymer known for its slow biodegradation rate and high mechanical strength [9]. Both polymers are interesting to elaborate food packaging materials due their biocompatibility, biodegradability, good chemical and thermal stability and non-toxic nature [8, 9].

Electrospun nanofibers can be applied in active food packaging, due to their capacity for controlled release of encapsulated bioactive molecules. When compared with the traditional casting films, they are more sensitive to the changes of the surrounding environment due to the structural characteristics, which facilitate them to achieve functional activity in the food packaging application [10, 11]. Nanofibers are fibrous nanocarriers that can be synthesized from natural or synthetic polymers. They can be produced by electrospinning, a technology for obtaining continuous polymer fibers with a diameter ranging in the nanometer scale. The process employs high strength electric field to produce ultra-fine fibers from a polymeric solution incorporated with a drug accelerated towards a collector [12, 13].

These nanostructures present unique properties, such as a high surface area-to-volume ratio, high porosity, low density, small pore size stability, permeability, and morphology that resembles an extracellular matrix. They also have high mechanical strength, making them excellent platforms for drug delivery purposes. Nanofibers can deliver a significant amount of drug and provide effective interaction of desired compound at the site of action due to a larger surface area [13, 14].

PVA and PCL nanofibers have been described as suitable materials for development of active packaging by incorporating either antimicrobial [14, 15] or antioxidant substances [16, 17]. However, studies related to this topic are limited and nanofibers showing multiple biological activities are barely reported. In this work, PVA and PCL nanofibers loaded with LBA were manufactured for the first time and their antimicrobial activity, antioxidant activity and toxicology evaluation were achieved. In this regard, nanofibers incorporating LBA could be expected as useful active materials showing both antimicrobial and antioxidant properties.

Therefore, the aim of this study was to obtain electrospun nanofibers with antibacterial and antioxidant activities through incorporation of LBA, and perform detailed toxicological evaluation and characterization of physical, thermal, and mechanical properties.

2 Materials and methods

2.1 Electrospun nanofibers

Electrospinning was carried out as described previously [14] with minor modifications. For the elaboration of nanofibers, poly(vinyl alcohol) (PVA; MW 146–186 kDa) was dissolved in ultrapure water (Millipore, Billerica, MA, USA) at 85 °C, and poly(ε-caprolactone) (PCL; MW 80 kDa) dissolved in tetrahydrofuran:dimethylformamide (THF:DMF, 1:1, v/v). Both polymers and organic solvents were purchased from Sigma-Aldrich (St. Louis, MO, USA).

Polymeric solutions containing 100 mg/mL (10%, w/w) and 150 mg/mL (15%, w/v) of either PVA or PCL were prepared, with addition of 1.5 mg/mL LBA (Sigma-Aldrich, 97% purity). Nanofibers without LBA were produced as a control. The formulations are detailed in Table 1.

Preliminary tests were carried out varying the voltage from 10 to 25 kV, feeding rate from 0.05 to 0.1 mL/min, and using acetone or THF:DMF as solvent for PCL. After optimization, the following parameters were applied to the electrospinning equipment (BR Robotics, Porto Alegre, Brazil): 3 mL of injected polymeric solution; voltage of 20 kV; feeding rate of 0.08 mL/min; inner needle diameter of 0.5 mm; distance to the collector 9 cm. The nanofibers were collected on

an aluminum plate (15 × 15 cm). The process was developed at 25 ± 1 °C. The resulting nanofibers were dried overnight for elimination of any residual solvent.

2.2 Antimicrobial activity

The microorganisms *Listeria monocytogenes* (ATCC 7644), *Staphylococcus aureus (*ATCC 25923), *Escherichia coli* (ATCC 25922) and *Salmonella enterica* serovar Enteritidis (ATCC 13076) were used to the antimicrobial assay.

The antimicrobial activity of the samples was determined using the agar diffusion assay as described previously [14]. Nanofiber samples were cut into disks (approximately 6 mm), sterilized under UV light for 30 min each side. The assay was performed using cells suspension (10^8 CFU/mL) in saline solution (9 g/L NaCl) followed by inoculation with a swab onto brain heart infusion agar plates (BHI; Merck, Darmstadt, Germany). Inhibition diameters were measured after overnight incubation at 37 ± 1 °C. PVA and PCL nanofibers prepared from polymer solution without LBA were also tested as negative control. Experiments were performed in triplicate.

2.3 Antioxidant activity

The antioxidant activity of the nanofibers was evaluated through the antioxidant potential regarding the quenching of 2,2′-azinobis-(3-ethylbenzothiazoline-6-sulfonic acid) (ABTS, %) using the method described previously [18]. The ABTS cationic radical solution was prepared by reacting 5 mL of ABTS solution (7 mM) with 88 µL of $K_2S_2O_8$ solution (140 mM). Previously the mixture remained in the dark for 12–16 h, at room temperature (25 ± 1 °C). For the tests, the ABTS radical solution was diluted in phosphate-buffered saline (PBS; pH 7.4) until it reached an absorbance of 0.700 (± 0.02) at 734 nm.

An extraction protocol was performed for the nanofibers as described previously with minor modifications [19]. Pieces of nanofibers (5 mg) were added to 4 mL of bicarbonate/carbonate buffer solution (0.2 M, pH 9.5) and vortexed during 3 min. Subsequently, the suspensions were sonicated during 15 min in an ultrasonic bath and centrifuged for 15 min at 3000 g. LBA solution (1.25 mg/mL) was also tested for comparison with LBA encapsulated in the nanofibers.

The samples (nanofiber extracts and free LBA) were added to 1 mL of the ABTS radical solution and the absorbance at 734 nm was measured after 10 min. The results were calculated and expressed using the following equation:

$$\text{Radical capture}\,(\%): \quad \left[(\text{Ac}-\text{As})/\text{Ac}\right] \times 100$$

where Ac and As is the absorbance of the control and the sample, respectively. Experiments were performed in triplicate.

2.4 Characterization of nanofibers

2.4.1 Scanning electron microscopy (SEM)

The morphology of the nanofibers was observed by SEM using a Zeiss EVO MA10 microscope (Zeiss, Jena, Germany). Firstly, the samples were coated with a layer of gold by cathodic spraying. Images were obtained at an accelerating

Table 1 Nanofiber formulations

Nanofiber	Formulation
A—PVA10 (control)	PVA 10% (w/v), ultrapure water
B—PVA15 (control)	PVA 15% (w/v), ultrapure water
C—PVA10 + LBA	PVA 10% (w/v), ultrapure water, 1.5 mg/mL LBA
D—PVA15 + LBA	PVA 15% (w/v), ultrapure water, 1.5 mg/mL LBA
E—PCL10 (control)	PCL 10% (w/v), THF:DMF (1:1, v/v)
F—PCL15 (control)	PCL 15% (w/v), THF:DMF (1:1, v/v)
G—PCL10 + LBA	PCL 10% (w/v), THF:DMF (1:1, v/v), 1.5 mg/mL LBA
H—PCL15 + LBA	PCL 15% (w/v), THF:DMF (1:1, v/v), 1.5 mg/mL LBA

voltage of 10 kV. The average fiber diameter was determined from the SEM images, and around 100 fibers were analyzed for each treatment using ImageJ software [20].

2.4.2 FTIR analysis

To investigate the chemical structure of the nanofibers, Fourier transform infrared (FTIR) spectra were obtained using a FT-IR spectrometer (Thermo iN10, USA) with a wavenumber range of 600 cm^{-1} to 4000 cm^{-1} with a resolution of 4 cm^{-1}.

2.4.3 Thermogravimetric analysis (TGA)

The thermal stability of the nanofibers was verified using a thermogravimetric analyzed model TGA Pyris 1 (PerkinElmer, USA). The samples were heated in platinum pans from 30 to 850 °C, at a rate of 10 °C/min, under a nitrogen gas atmosphere with a flow rate of 20 mL/min as described previously [11, 14].

2.4.4 Differential scanning calorimetry (DSC)

The DSC assay was performed using a DSC 8500 apparatus (PerkinElmer, USA). Samples of approximately 11 mg were placed in aluminum containers and heated from 20 to 200 °C, with a heating rate of 10 °C/min, under a nitrogen gas flow of 20 mL/min. An empty container sealed with a lid was used as a sample reference. The crystallinity for nanofibers was calculated using the following equation:

$$Xc = \Delta Hm/\Delta Hc$$

where, ΔHm = enthalpy of fusion (J/g) and ΔHc = melting enthalpy, considering the melting enthalpy of 100% crystalline PVA is 159 J/g and of 100% crystalline PCL is 81.6 J/g.

2.4.5 Mechanical properties

The mechanical properties of the nanofibers were determined using a TA.XT Plus Texture Analyzer equipment (Stable Microsystems, UK) based on ASTM D638-14 [21]. The nanofibers were cut into strips $40 \times 10 \times 0.1$ mm (length × width × thickness). The experiment was conducted at room temperature applying a preload force of 0.049 N and a controlled force rate of 0.8 mm/s and the initial grip separation was set at 200 mm. The data for the maximum strain (ε, elongation at break, %), the maximum stress (σ, tensile strength, MPa) and elastic modulus (*E*, Young's modulus, MPa) were determined from the stress–strain curves. Tests were replicated at least three times for each sample.

2.5 Hemolysis assay

The hemolysis assay was performed as described previously [14]. Aliquots (1 mL) of defibrinated sheep blood (NewProv, Pinhais, Brazil) were added to 4 mg of each nanofiber sample and 1 mL PBS (pH 7.4). After incubation for 60 min at 37 °C, samples were centrifuged at 900 g for 10 min and 1 mL of the supernatant was collected. The amount of hemoglobin released was determined by reading the absorbance at 540 nm. Triton X-100 (0.1%, v/v) was used as a positive control (C+), and considered as 100% hemolysis and PBS was considered the negative control (C–), and considered as 0% hemolysis. The same amount of LBA (4 mg) was tested for comparison with the encapsulated form (nanofibers). Hemolytic activity was calculated using the following equation:

$$\text{Hemolytic Activity} = (\text{Aa} - \text{An})/(\text{Ap} - \text{An}) \times 100\%$$

where Aa, An and Ap is the absorbance of the sample, negative control, and positive control, respectively. Experiments were performed in triplicate.

2.6 Toxicology assessment

2.6.1 Mutagenicity assay

The Ames mutagenicity test was performed by the pre-incubation protocol [22], with minor modifications. The *Salmonella* Typhimurium strains, TA98 (ATCC®, Number BAA-2720™) and TA100 (ATCC®, Number BAA-2720™), were used to detect frameshift mutation and base pair substitution respectively. First, LBA, PVA10 and PVA10 + LBA nanofibers were subjected to an extraction protocol where it was dissolved in ultrapure water (Millipore, Billerica, MA, USA) during 24 h [19]. Four concentrations were tested (0.078, 0.1562, 0.3125 and 0.625 mg/plate) in absence of metabolic activation (-S9). The supernatant (PVA10 + LBA extraction) were tested in five concentration (6.25 to 100%, 50 µL/plate) in absence of metabolic activation (-S9). The vehicle (ultrapure water) was used as the negative control. The positive controls were 4-nitroquinoline N-oxide (4-NQO, 100 µg/plate), and sodium azide (SAZ, 5 µg/plate), for TA98 and TA100 respectively. The supernatants (LBA, PVA10 and PVA10 + LBA extraction) were also tested in five serial dilutions (100 to 6.25%, 50 µL/plate) in presence of metabolic activation (addition of S9 fraction), and the positive control used was 2-aminofluorene (2-AF) for both TA98 and TA100.

Both TA98 and TA100 strains were incubated overnight with nutrient broth at 37 °C for exponential growing phase. A sample of 100 µL of each strain (approximately 10^9 cells/mL) were incubated with LBA, PVA10 and PVA10 + LBA or controls for 30 min in absence of metabolic activation. In parallel, LBA, PVA10 and PVA10 + LBA or controls were incubated with 100 µL of each strain for 30 min in presence of metabolic activation. After, samples were mixed with 2 mL of top-agar (0.6% agar, 0.5% NaCl, 5 mM histidine and 50 mM biotin) and mounted in minimum medium agar plates (1.5% agar, Vogel-Bonner salts and 2% glucose). Plates were incubated at 37 °C from 48 to 72 h before the final colony counting.

2.6.2 Cell survival measurement

Cell survival was accessed by the colony formation assay as described by ISO 10993–05 [23]. This assay measures cell survival by ability of a single cell to grow into a colony [24]. The V79 cells were maintained in MEM medium with 10% fetal bovine serum. Cells were seeded in 6-well plates in low density (200 cells per well) and incubated 24 h prior to the exposure. The nanofibers were extracted in culture media for 24 h (37 °C) prior to the exposure and the supernatants were tested in five serial dilutions (1:10, from 100 to 0.01%). The negative control was high-density polyethylene (HDPE) and the positive control was natural latex, both submitted to the same extraction process. Cells were incubated during 7 days, washed with PBS, and then colonies were stained with 5% Giemsa solution. The results were expressed in % of survival calculated by colony counting.

2.6.3 Cell viability analysis

Cell viability was analyzed by the MTT assay according to the ISO 10993-05 [23]. This method evaluates cell viability by quantitative colorimetric measure in mammalian cell by the metabolization of the tetrazolium salts that are reduced to formazan products in purple [25]. L929 cells were maintained in MEM media with 10% fetal bovine serum. Cells were seeded in a 96 well plate and incubated 24 h prior to the exposure. The nanofibers were extracted in culture media for 24 h (37 °C) and the supernatants were tested in six serial dilutions (1:2, from 100 to 3.12%). After 24 h exposure, cells were washed and incubated 2 h with MTT salts solution. The reduced MTT (formazan) was dissolved with 50 µL isopropanol in each well and absorbance at 570 nm was measured using a microplate reader (Perkin Elmer, Inspire).

2.6.4 Agar diffusion cytotoxicity test

The capacity of nanofibers to leach and induces cytotoxicity was evaluated by the agar diffusion cytotoxicity test [26]. SIRC cells derived from rabbit corneal were maintained in MEM media with 10% fetal bovine serum, 1,000 U/mL penicillin and 100 µg/mL streptomycin, at 37 °C with 5% CO_2 condition. Cells were seeded in 6 well plate in a density of 5×10^5 per well 24 h prior to the exposure. An agar overlay containing bacto agar (1%, w/v), neutral red (0.005%, w/v) and culture media was prepared and cells were coated with the solution. Results were expressed according to the reactivity area diameter from the nanofiber. The following classification is according to the ISO 10993 [23]: 0, no reactivity; 1, malformed

cells only around of contact; 2, 0 to 0.5 mm in diameter of malformed cells, 3, 0.5 to 1 mm in diameter of malformed cells; 4, > 1 mm in diameter of malformed cells.

2.7 Statistical analysis

The descriptive statistics were performed for the *in vitro* assays based on the mean average method and the standard errors were calculated. The toxicological assessment (except hemolysis assay) was evaluated by analysis of variance (ANOVA).

3 Results and discussion

3.1 Electrospun nanofibers

Eight nanofiber formulations were prepared from spinning solutions containing 10% and 15% (w/v) of either PVA or PCL, with the presence or absence of LBA in the formulation (Table 1). The electrospinning conditions allowed the production of nanofiber mats from all formulations tested. Each nanofiber mat contained approximately 22.5 mg LBA/g. The biological and physicochemical properties and toxicological evaluation of the obtained nanofibers are presented in the next sections.

3.2 Antimicrobial activity

The antimicrobial activity was evaluated by agar diffusion test and the results are summarized in Table S1 and Fig. S1. PVA nanofibers showed antimicrobial activity against *S. aureus*, while no inhibitory effect was observed against the other bacteria tested. Moreover, the PCL nanofibers did not show antimicrobial activity under the conditions tested.

The mechanism of action of LBA involves the loss of cell membrane integrity, inhibition of DNA and protein synthesis, and the induction of oxidative stress in both Gram-positive and Gram-negative bacteria. Furthermore, it causes an increase in the permeability of the outer membrane, causing hypo-osmotic shock in Gram-negative bacteria. Specifically, LBA negatively affected the growth of *S. aureus* in a dose-dependent manner, damaging the integrity of the cell membrane [3, 5]. The lack of inhibitory effect on some bacteria observed in this work may be partially due to the quantity of LBA in the nanofibers, as the LBA amount was around 22.5 mg/g. The MIC values described for *S. aureus* are 15 mg/mL [5], but can be higher for *Listeria*, *Salmonella*, and *E. coli* and also some *S. aureus* strains [2, 3].

The absence of antimicrobial activity for PCL nanofibers may also indicate a very low release rate that could be associated to the polymer degradation profile and nature. PCL is quite stable polymer as it has a few numbers of ester bonds per monomer, which results in slower degradation and release rates [27]. Therefore, the slow degradation of PCL could be delaying the release of LBA, resulting in the absence of antimicrobial activity on agar assays. Similar effect was previously observed for PCL nanocapsules containing antimicrobial peptides [28].

The inhibitory activity of bare PVA hydrogels was observed against *S. aureus* and *Bacillus subtilis* through the agar well diffusion method, suggesting that this polymer can hinder bacterial growth [29]. In another study, PVA-based nanofibers intended for wound dressing reduced the number of *S. aureus* colonies due to the fiber structure and porosity that favor the process of bacteria entering the nanofiber [30]. Similarly, the inhibitory effect of control PVA nanofibers (Table S1) can be associated with the efficiency of bacterial removal by this material. Moreover, nanofibers loaded with LBA resulted in higher inhibition zones (Table S1 and Fig. S1), which could be attributed to the antimicrobial activity of LBA.

Moreover, it is worth highlighting that the distribution of compounds in the nanofiber at the time of electrospinning may not have been uniform, as the jet is not controllable, thus a certain area of the nanofiber may have had a lower concentration of antimicrobial while another area may have remained with an accumulation of antimicrobial. Thus, the uneven distribution of the active compound possibly interfered with the antimicrobial activity.

3.3 Antioxidant activity

The antioxidant potential of the nanofibers was evaluated by the ABTS radical scavenging activity. The formulation PVA15 + LBA showed higher activity among all formulations, reaching 37.6% (798.7 µM TEAC). The other nanofibers showed similar activity, ranging from 32.9% to 36.9%, corresponding to 690.3 and 761.2 µM TEAC, respectively (Fig. 1).

The LBA solution showed activity of 33.9% (715.33 µM TEAC), while control nanofibers showed no significant ABTS scavenging activity.

Because absorption of ABTS may occur by the large surface area of the nanofibers, these were subjected to an extraction protocol that was effective to evaluate antioxidant activity of nanofibers [19]. The high voltage used in the electrospinning process can be harmful to bioactive compounds, resulting in the loss of biological activities. However, the antioxidant activity of LBA was maintained in the electrospun fibers, similar to that observed for PVA-based nanofibers containing antioxidant substances like gallic acid at 2.5 and 5%, showing 34% and 42% ABTS radical scavenging, respectively [31]. In other studies, 12% PCL nanofibers containing 3% curcumin achieved a radical scavenging of 31.5% in the ABTS assay [32], while 15% PVA nanofibers containing 0.2% phycocyanin showed 24.68% elimination of the ABTS radical [33]. The authors suggest a possible application of those materials as active packaging with antioxidant properties.

The ABTS assay, which is widely used for determination of antioxidant activity of biological samples, involves the reaction between the antioxidant and ABTS radical cation ($ABTS^{\cdot+}$), through a hydrogen atom transfer reaction or single electron transfer reaction mechanisms [34]. In this regard, LBA is likely to act as an H donor promoting the antioxidant effect. The antioxidant properties of LBA-containing nanofibers may be relevant for active packaging applications, since lipid oxidation can cause important losses of sensorial and nutritional quality of foods and even may lead to the formation of toxic aldehydes. Antioxidant packaging can extend the shelf life of foods by retarding the rate of oxidation reactions [6, 7]. Although reports correlating the ABTS activity of packaging materials with antioxidant effect in real foods are scarce, polyethylene terephthalate (PET) and low density polyethylene (LDPE) films containing *Salvia officinalis* L. and *Laurus nobilis* L. extracts with 50% ABTS scavenging caused reduction of lipid oxidation in fried potatoes [35].

3.4 Characterization of nanofibers

Controlling the physicochemical characteristics of nanofibers is one of the main difficulties during the electrospinning process. The physicochemical properties of nanofibers can be influenced by a series of variables, including the polymeric solution (concentration effects, conductivity, solvent systems, surface tension, dielectric constant, and volatility), the environment, the collector (geometry and material), the applied potential (voltage, tip polarity), the feed rate, the capillary tip and the distance between the tip and the collector [12]. Due to this, it is essential to characterize the physical, thermal, and mechanical properties of nanofibers obtained by electrospinning.

3.4.1 Scanning *electron* microscopy (SEM)

The SEM images show the morphology of PVA and PCL fibers obtained by electrospinning (Fig. 2). The histograms showing the distribution of fiber diameters are presented for each nanofiber (Fig. 2) and average diameters were determined for all nanofiber formulations (Table S2). Detailed SEM images are presented for the PVA10 + LBA nanofiber (Fig. S2), which was selected for cytotoxicity assays as discussed below.

The PVA and PCL fibers were uniform and well-formed structures for both control and LBA nanofibers. The morphology was typical string-like. In PVA fibers, there was no formation of beads, granules, or agglomerations, showing uniformity along the fibers and they were essentially well-aligned fibers. The PCL ones present some agglomerations

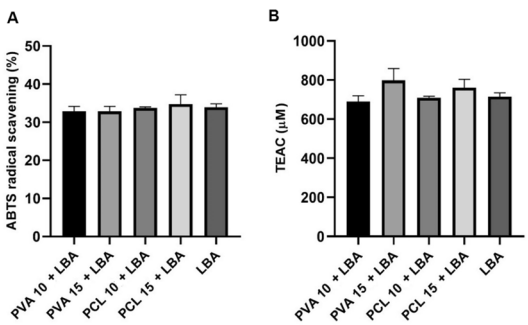

Fig. 1 Antioxidant activity of PVA and PCL nanofibers. The nanostructures were subjected to an extraction protocol and the antioxidant activity was measured by scavenging of the ABTS radical as detailed in Materials and Methods. Results are expressed as % radical scavenging (**A**) and Trolox equivalents (**B**). LBA (1.25 mg/mL) was also tested for comparison with the encapsulated form (nanofibers). Data represent mean ± standard deviation of three independent experiments

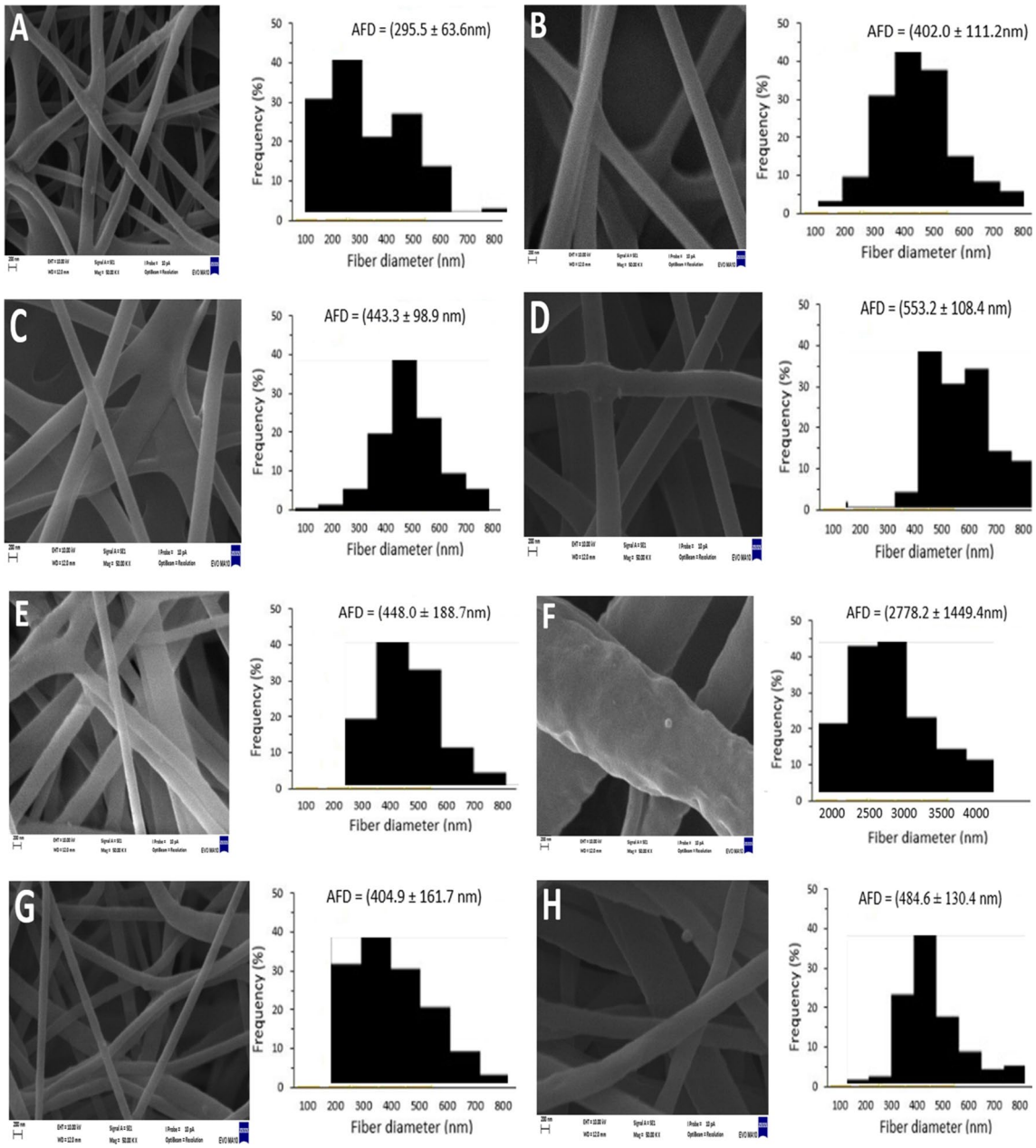

Fig. 2 Scanning electron microscopy images of the nanofibers (magnification 50,000×). **A** PVA10; **B** PVA15; **C** PVA10 + LBA; **D** PVA15 + LBA; **E** PCL10; **F** PCL15; **G** PCL10 + LBA; **H** PCL15 + LBA. The histogram images show the frequency distribution and the average diameter (nm) of the fibers measured using ImageJ software

along the fibers, less aligned fibers (some overlapping and coiled fibers), but there was no formation of beads. A certain roughness was observed for PCL fibers (Fig. 2). The control PVA nanofibers had a smaller average diameter than the PCL nanofibers, and presented better-formed fibers (Fig. 2) with a more uniform distribution and average diameter (Fig. 2 and Table S2).

The control PVA nanofibers had a smaller average diameter as compared with PVA-LBA fibers, indicating that the addition of LBA increased the average size of the fibers. As for the PCL nanofibers, the control nanofibers showed a larger average diameter compared to the fibers with LBA addition. Furthermore, LBA improved the appearance of the fibers, leaving them better distributed and aligned. However, the control PCL15 nanofiber did not show good distribution. These fibers showed quite a large variation in their diameter, and agglomerated and tangled fibers as well.

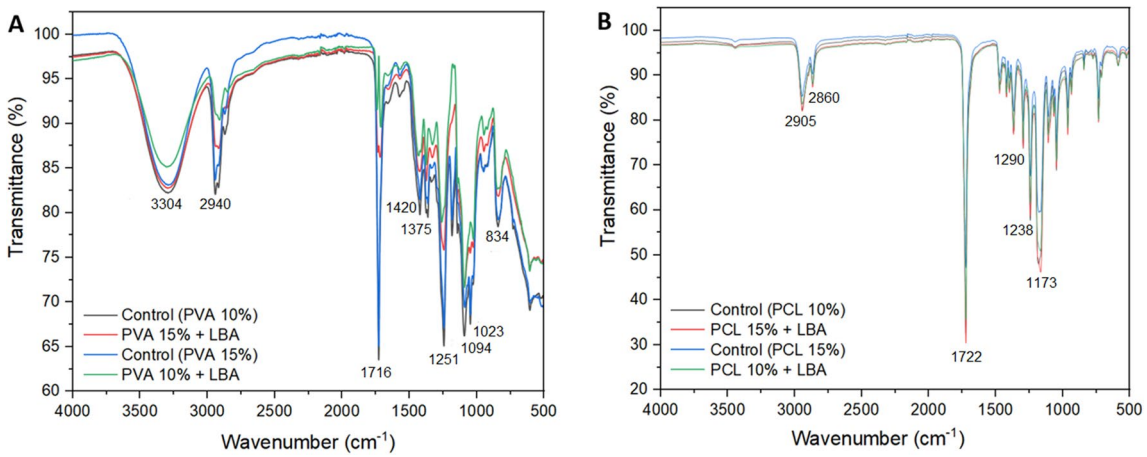

Fig. 3 FTIR spectra of PVA nanofibers (**A**) and PCL nanofibers (**B**)

The incorporation of LBA changes the ionic strength of the solution, which possibly caused changes in the diameter of the fibers. Another factor that affects fiber diameter is increased filler density, subjecting the jet to stronger stretching forces, resulting in smoother, thinner fibers. Furthermore, the formation of intermolecular hydrogen bonds of polymers and the repulsion between the molecules of the added compounds can also promote the formation of more uniform nanofibers [36, 37].

Factors such as viscosity and conductivity can affect the morphology and diameter of nanofibers. When the solvent does not evaporate before fiber deposition, the jets can coalesce, forming materials with different morphologies [14, 38]. Furthermore, smooth nanofibers are usually formed when all ingredients in the formulation have good miscibility. A good polymer–solvent interaction, with a balance between surface tension and the solvent evaporation rate, contributes to the creation of homogeneous and defect-free nanofibers. Thus, the hydrophilic character of PVA may provide improved compatibility with LBA, resulting in more uniform electrospun fibers.

3.4.2 FTIR analysis

FTIR experiments were performed to determine possible polymer-LBA interactions. The FTIR results for the control nanofibers and nanofibers incorporating LBA are presented in Fig. 3. The wavenumber of each peak indicates the presence of a specific functional group in the sample. The FTIR spectra of PVA fibers showed typical bands at 3400–3200 cm^{-1} (stretching of the O–H groups), 2905 cm^{-1} (asymmetric stretching of the $–CH_2$ group), and peaks at 2939 cm^{-1} related to C–H stretching, 1420 cm^{-1} related to CH_2 stretching, and at 1094 cm^{-1} due to C–O–C stretching. These results are consistent with those found in chitosan and PVA nanofibers [37]. FTIR spectra of PCL nanofibers showed characteristic PCL peaks at 2905 cm^{-1} (asymmetric stretching of CH_2), 2860 cm^{-1} (symmetric stretching of CH_2), 1722 cm^{-1} (stretching of the carbonyl), 1290 cm^{-1} (C=O and C–C stretching), 1238 cm^{-1} (corresponding to C–O–C asymmetric stretching) and 1173 cm^{-1} (compatible with C–O–C symmetric stretching). These data are consistent with those found in nanofibers containing PCL [14, 39].

No relevant differences were observed between the FTIR spectra of the control nanofibers and the nanofibers containing LBA. This may indicate that there is no significant chemical interaction between the additive and polymers, which confirms the stability of the substances with their solid dispersion. Moreover, typical stretching signals of LBA at 2910 cm^{-1} (C–H), 1720 cm^{-1} (C=O) and 1070 cm^{-1} (C–O) [40], are probably overwritten by signals of the polymer matrix, as the relatively low concentration of the active molecule in nanofibers can prevent the identification of specific absorption bands [41].

3.4.3 Thermogravimetric analysis (TGA)

The thermal stability of the nanofibers was evaluated using thermogravimetric analysis. TGA analyzes are essential for estimating the thermal stability of materials [11]. The mass loss profiles as a function of temperature of LBA nanofibers are shown in Fig. S3.

Thermograms for LBA-containing nanofibers show three main weight loss stages caused by water evaporation and thermal degradation of polymer chains. For PVA nanofibers, a first weight loss (about 10%) occurred between 60 and 280 °C. For PCL nanofibers, a first weight loss (around 5%) occurred between 210 and 380 °C. This first stage could be attributed to water loss. The most significant weight loss (around 60%) for PVA occurred between 250 and 400 °C, and for PCL (around 85%) it occurred between 350 and 460 °C. This probably occurred due to the breakdown of polymer chain interactions, such as hydrogen bonds, dehydration of carbohydrates and the depolymerization process.

A third stage of weight loss was observed between 390 to 510 °C for PVA (around 20%) and between 450 to 600 °C for PCL (around 10%), which may be mainly associated with the degradation of polymers. For PVA, a fourth stage of weight loss (around 10%) was observed from 510 °C until complete decomposition. These results are consistent with those found by other authors for PCL and PVA nanofibers [41, 42].

3.4.4 Differential scanning calorimetry (DSC)

DSC analysis was performed to understand the physical state of the compounds in the electrospun nanofibers. DSC analysis is essential for estimating possible changes in the intermolecular structure of compounds [11]. Table 2 presents the main thermal parameters derived from the DSC thermograms, which are displayed in Fig. S4.

A typical endothermic melting peak for PCL at around 55 °C was observed in the thermograms of control PCL10 and PCL15, and PCL15 + LBA nanofibers. For PCL10 + LBA nanofibers, the endothermic peak was around 60 °C, indicating that the PCL fibers obtained had a crystalline structure. For the control PVA10 and PVA15 nanofibers, the endothermic peak was 42.44 °C and 35.72 °C, respectively. These values were around 58 °C and 68 °C for the PVA10 + LBA and PVA15 + LBA nanofibers, respectively.

A slight variation in melting peaks (intensity and position of endothermic peaks) indicates that the solvents used in the formulations can affect the thermal behavior of PCL and PVA. These effects may be related to solvent properties, including different interactions with certain polymers and the degree of volatility. Rapid evaporation of the solvent is necessary for the formation of nanofibers during electrospinning, and this rate can influence polymer crystallization [14].

Furthermore, the change in the melting peak and enthalpy can be related to the plasticizing effect of the added compound, which increases the mobility of the polymer matrix chain. The shift of the melting peak can be related to the intermolecular interactions between components, where stronger interactions led to a greater shift of the melting peak at high temperature. Therefore, it can be suggested that the incorporation of LBA changes the ionic strength of the solution. Furthermore, viscosity and conductivity may also have been responsible for these changes [11, 36].

The degree of crystallinity of the control PVA10 nanofiber was 10%, changing to 4.8% with the addition of LBA. The same occurred with the degree of crystallinity of the PVA15 nanofiber, reduced from 35% for the control nanofiber to 3.7% with the addition of LBA. Similar influence of LBA on the degree of crystallinity was also observed for PCL nanofibers, where LBA-containing nanofibers showed lower values as compared with control nanofibers (Table 2).

The presence of some additives could reduce the space available for crystal growth, reducing the crystallinity of the nanofibers. Therefore, it can be suggested that LBA possibly hindered the diffusion of PVA and PCL chains and contributed to changes in crystallinity in the polymer. Crystallinity is also affected by the electrostatic field, the time of crystallization

Table 2 Thermal parameters of PVA and PCL nanofibers derived from DSC thermograms

Formulation	Thermal Parameter [a]			
	*T*onset (°C)	*T*m (°C)	Δ*H*m (J/g)	χ_c (%)
A—PVA10 (control)	42.44	57.20	15.92	10
B—PVA15 (control)	35.72	65.70	56.74	35
C—PVA10 + LBA	58.82	70.41	7.64	4.8
D—PVA15 + LBA	68.57	85.66	5.97	3.7
E—PCL10 (control)	54.90	59.00	71.70	87
F—PCL15 (control)	55.08	59.70	70.97	87
G—PCL10 + LBA	62.60	67.44	36.45	45
H—PCL15 + LBA	54.98	58.77	55.52	68

[a] *T*onset = beginning of melting temperature; Tm = melting temperature; Δ*H*m = enthalpy of fusion; χ_c = crystallinity, calculated by $\chi_c = \Delta Hm/\Delta Hc$, considering that the melting enthalpy of 100% crystalline PCL is 81.6 J/g and 100% crystalline PVA is 159 J/g

during the flight of the jet and by the voltage applied to obtain the nanofibers, since the crystallinity can decrease as the voltage increases. The absence of a detectable crystalline peak for LBA in the nanofibers suggests that the substance was molecularly dispersed within the polymeric matrix or was present within the fibers in an amorphous state [14, 36].

3.4.5 Mechanical properties

To verify the effects of LBA addition on the mechanical properties of the PVA and PCL electrospun nanofibers, stress–strain curves were obtained using a texture analyzer (Fig. S5). The values of Young's modulus, tensile strength, and maximum strain (elongation at break, %) were determined (Table 3). While the Young's modulus increased in PVA nanofibers containing LBA, the values decreased from about 20 MPa to less than 10 MPa for PCL nanofibers with addition of LBA, indicating a decrease in stiffness of the nanofiber mats [43]. The tensile strength increases in PVA nanofibers containing LBA, suggesting the segmental motions of neighboring polymer chains could be improved due to the compatibility with the additive. Excepting for PVA10 nanofibers, the values of elongation at break were similar among control nanofibers and samples with LBA (Table 3). These changes in mechanical properties can be related to the dispersion of the additive, since the degree of interaction between LBA molecules and polymers may influence the formation of agglomerates, thus affecting the nanofiber structure [44, 45]. Furthermore, the alignment of the nanofibers during the deposition on the collector may also have been uneven depending on the sample, resulting in a different conformation, and influencing the mechanical properties [36].

The tensile strength of low-density polyethylene (LDPE) films is about 9–10 MPa and their elongation at break is no less than 200%, while the elongation at break is 100% and the tensile strength of polypropylene is 31–41 MPa [46, 47]. Some of the PVA and PCL nanofibers showed elongation at break similar to those polymers currently used as food packaging materials, but lower values of tensile strength. Due to their structural features, nanofibers are not compact materials and may result limited mechanical and barrier properties as compared to conventional films produced by casting or thermal extrusion. However, the large surface area to volume ratio make nanofibers excellent platforms for delivery of bioactive compounds [12, 48].

In general, it is difficult to achieve all the desirable properties required for efficient packaging using a single material. Therefore, materials with improved features can be obtained by combination of polymers, multilayer films, and/or using nanocomposites [48]. These strategies can be useful for preparing packaging materials based on easily water-soluble polymers such as PVA. For example, active fibers with potential food packaging application can be formulated with PVA/chitosan/cinnamaldehyde [8] and PVA/gelatin/pine honey [16], which showed improved water barrier and antioxidant properties. In another study, a multifunctional nanocomposite incorporating titanium dioxide and apple peel extract into a PVA/cellulose nanocrystal matrix was developed for food packaging applications [49]. This material provided an exceptional UV barrier and outstanding antioxidant and antimicrobial properties, protecting fresh samples of cherry tomatoes and potatoes from external influences and extending their shelf life in food packaging tests.

Table 3 Mechanical properties of PVA and PCL nanofibers

Formulation	Young's modulus (MPa)	Tensile strength (MPa)	Elongation at break (%)
A—PVA10 (control)	22.9 ± 2.8	14.93 ± 1.88	103 ± 22
B—PVA15 (control)	12.2 ± 1.3	3.36 ± 0.84	41 ± 4
C—PVA10 + LBA	32.4 ± 3.5	5.08 ± 0.10	18 ± 6
D—PVA15 + LBA	23.4 ± 6.6	6.06 ± 2.29	39 ± 15
E—PCL10 (control)	20.7 ± 3.6	6.24 ± 0.73	42 ± 6
F—PCL15 (control)	19.9 ± 1.9	1.32 ± 0.14	138 ± 38
G—PCL10 + LBA	8.7 ± 2.2	2.79 ± 0.86	47 ± 10
H—PCL15 + LBA	4.8 ± 1.1	6.07 ± 1.16	146 ± 15

Data represent mean ± standard deviation of three independent experiments

3.5 Toxicological assessments

The potential toxicity of nanofibers was assessed by the hemolysis test and the PVA10 + LBA was selected for further cytotoxicity evaluation due to some features, including antimicrobial and antioxidant activity, smaller fiber diameter and less polymer added to the formulation.

3.5.1 Hemolysis assay

In vitro determination of hemolytic properties often constitutes an initial step in cytotoxicity assessments. This is a common and important method for preliminary evaluation of cytotoxicity of chemicals, drugs, materials and medical devices [50]. The nanofibers tested presented a degree of hemolysis below 2% (Fig. 4). This assay showed that PVA and PCL nanofibers containing LBA caused no significant lysis of erythrocytes, and could be considered as non-hemolytic materials. Likewise, the hemolytic activity was low for LBA and control nanofibers.

Similar results were found in other studies. PCL nanofibers incorporated with natamycin resulted in low hemolytic degree ranging from 1.2 to 6.5% [14]. Other nanostructures, such as PCL nanofibers containing docetaxel doped ZnO nanoparticles, also showed low hemolytic rates [51]. These studies reinforce the good biocompatibility, biodegradability and non-toxicity of nanofibers, enabling them as a suitable biomaterial.

Materials with a hemolysis percentage below 2% are considered non-hemolytic materials, while materials with a hemolysis rate above 5% are considered hemolytic. When the degree of hemolysis is between 2 and 5%, they are classified as slightly hemolytic. A hemolysis rate up to 5% hemolysis is considered as tolerable for biomaterials [14, 52].

3.5.2 Toxicological assessment

The results of Ames test indicate that LBA, PVA10 and PVA10 + LBA nanofibers did not induce mutagenicity in TA98 and TA100 strains. Concerns regarding nanomaterial hazard potential includes the genotoxicity evaluation of the polymers and the encapsulated compounds [53]. Genotoxicity refers to a substance potentially harmful for the genetic material and may be induced, but not necessarily, by mutagenic effect [54]. Mutagenicity is a genotoxic event transmissible after cell replication and may involve a gene segment (point mutation) or a whole chromosome. The Ames test detect point mutations of exogenous substances capable of reverting mutations in histidine genes of *Salmonella* Typhimurium, restoring the ability of the bacteria to synthesize the amino acid [22].

In the range of concentrations tested, LBA caused no significant increase in the mutagenic index of TA98 and TA100 strains, but a minor cytotoxic induction in the highest dose for TA100 (Fig. S6). Since PVA was the polymer used to assembly the nanofibers, the strains TA98 and TA100 were also tested in presence of extract of PVA10 nanofiber. The mutagenic index for all concentrations tested of PVA10 extract was similar to that observed for the negative control (vehicle), showing no mutagenic induction (Fig. S7). At this point, both strains were evaluated in absence of metabolic

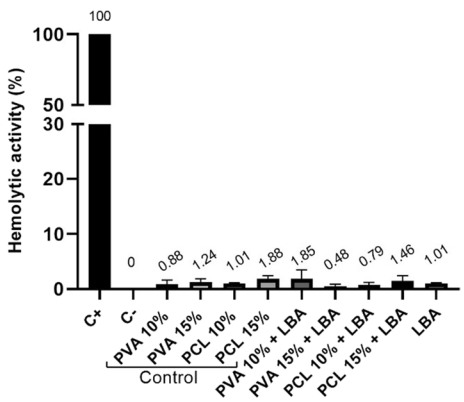

Fig. 4 Hemolytic activity of PVA and PCL nanofibers. Samples were incubated for 60 min with erythrocytes and released hemoglobin was measured at 540 nm. Triton X-100 was used as a positive control (C+) and represents 100% hemolysis. PBS was used as a negative control (C–) being considered 0% hemolysis. Data represent mean ± standard deviation of three independent experiments

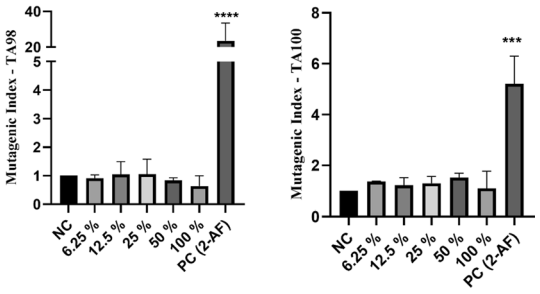

Fig. 5 Mutagenicity of PVA10 + LBA nanofiber extractions tested in TA98 and TA100 strains in presence of metabolic activation (+ S9). NC, negative control (vehicle); 6.25% to 100% (% of PVA10 + LBA extract – 50 µL/plate); PC (2-AF), positive control (100 µg/plate). Data represent mean ± standard deviation of three independent experiments. Mutagenicity were expressed by mutagenic index and significance calculated by one-way ANOVA Dunnett's multiple comparison test: ***$p < 0.001$; ****$p < 0.0001$

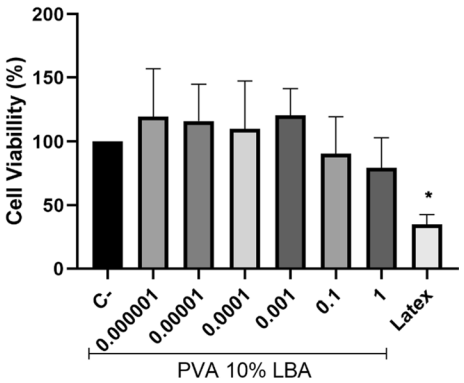

Fig. 6 Cellular viability assay in L929 cell line. Cells were treated for 24 h with increasing concentrations of PVA10 + LBA extracts and cell survival was assessed by the MTT assay. Data represent mean ± standard deviation of at least three independent experiments performed in duplicate. *P* values relative to the untreated control (C–) cells were calculated using one-way ANOVA Dunnett's multiple comparison test: *$p < 0.05$

activation and the highest doses of LBA or PVA10 + LBA tested showed no cytotoxic induction for the *Salmonella* strains and no increase of mutagenic index.

Lastly, the extract of PVA10 + LBA nanofiber was tested for mutagenicity in TA98 and TA100 strains in presence of metabolic activation. Interestingly, the assembly nanofiber did not increase mutagenic index for both strains (Fig. 5). TA98 and TA100 strains are used to detect frameshift mutation and base pair substitution respectively, and both caries the plasmid pKM101 producing the enhancement of inducible mutagenesis [55]. These results give an insight into safety assessment of the nanofibers and its encapsulated compound for possible application in food systems regarding the absence of point mutation induction as evaluated by the Ames test.

Furthermore, PVA10 + LBA was tested in different models for cytotoxicity potential. In vitro cytotoxicity tests has been used for varied cell toxicity measurements such as cell proliferation, cell viability and cellular metabolism [56–58]. In L929 cells, the extract of PVA10 + LBA caused no significant cytotoxicity regardless the dose, while the positive control (latex) highly decreased cell viability in the MTT assay (Fig. 6). The L929 is well established model for cytotoxicity evaluation (ISO 10993-05) [23], also used for the evaluation of nanomaterials intended to controlled release [59]. The MTT test evaluates cell viability by the metabolization of the formazan salt by mitochondria, providing a hint of how nanofibers can affect cellular metabolism. Therefore, this assay clarifies that this nanofiber composition does not induce cytotoxic effect as evaluated by mitochondrial activity.

Further, the ability of V79 cells to proliferate in contact with PVA10 + LBA extract was tested using the colony formation assay. After exposure, no decrease in cell proliferation was detected in all concentrations tested (Fig. 7). The cell proliferation was evaluated during long-term exposure, against the 24 h of MTT method. In the evaluation of cytotoxicity by metabolic systems, cells may overcome the underlying mechanisms remaining metabolically active. Therefore, is desirable to confirm the results using complementary methods to reach a more comprehensive response [60].

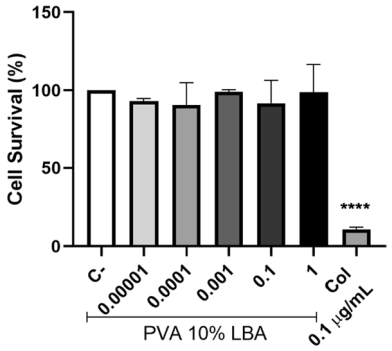

Fig. 7 Colony formation assay in V79 cell line. Cells were treated for 7 days with increasing concentrations of PVA 10 + LBA extracts and cell survival assessed by the colony formation assay. Data represent mean ± standard deviation of three independent experiments performed in duplicate. *P* values relative to the untreated control cells (C−) were calculated using one-way ANOVA Dunnett's multiple comparison test: ****$p < 0.0001$

Another approach to detect cytotoxicity is the evaluation of potentially leachable materials, therefore diffusing toxic substances [61]. Moreover, the production of nanofibers may presents hazard potential during processing and worker exposure [57]. To evaluate the capacity of nanofibers to produce cornea damage trough diffusion of potentially toxic substances, the agar diffusion cytotoxicity assay in SIRC cells was performed. The 24 h exposure to the negative control shows well-formed cells with high NR uptake, while the positive control shows malformed cells with no NR uptake in the damage zone extended above 0.5 mm in diameter (Fig. 8A, C, respectively). The PVA10 + LBA exposure, produced a few damaged cells around the point of contact, with a slight reduction of NR uptake (Fig. 8B), where damage zone is extended below 0.5 cm in diameter, indicating slight reactivity. This trace of cytotoxicity shows the ability of nanofibers to leach through the agar surface and affect cell viability, even resulting in low cytotoxic activity.

Considering that nanofibers could be commercially used as active materials, they probably have to meet regulatory requirements [62]. Therefore, this study followed the methods described in the ISO 10993-5:2009 Part 5, with minor modifications, to follow standard methods of analyses. In addition, the genotoxic compound identification provides a basis to understand the carcinogenicity potential. The Ames test provided a hint of non-mutagenic (non-genotoxic) effect of the nanofiber.

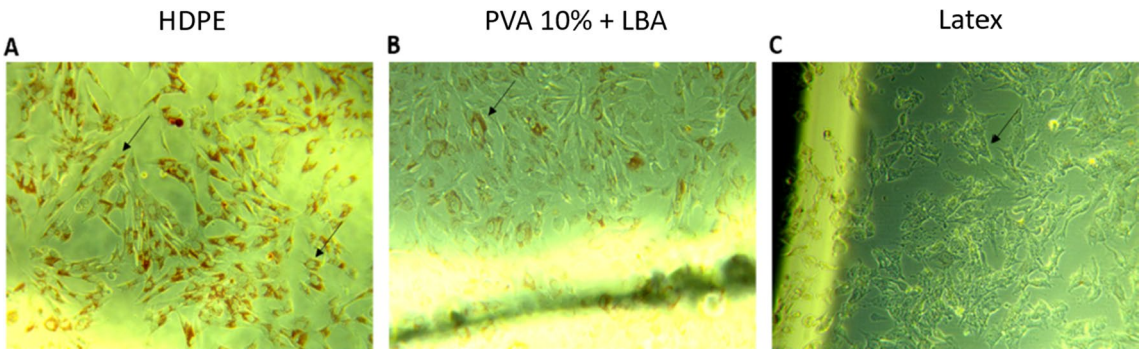

Fig. 8 Agar diffusion test in SIRC cells. **A** Cells exposed to negative control, high density polyethylene (HDPE), were cells shows a good morphology and high neutral red uptake. **B** Exposure do PVA10 + LBA lead to decreasing of neutral red uptake, but preserved morphology, the damage zone is extended below 0.5 mm in diameter. **C** Cells exposed to positive control (Latex), showing malformed cells with no neutral red uptake, where the damage zone extends above 0.5 cm in diameter. Microscopy images were captured from an inverted microscopy using a 10× objective lens

4 Conclusions

In the present study, PVA-LBA and PLC-LBA nanofibers were successfully obtained by electrospinning. The PVA-LBA nanofibers showed antimicrobial activity against *S. aureus*, while both PVA-LBA and PLC-LBA nanofibers presented antioxidant activity. The formulation PVA15 + LBA showed higher activity among all formulations, reaching 37.6% (798.7 µM TEAC). The average diameter increased when LBA was incorporated to PVA nanofibers, while the average diameter of the PCL nanofibers decreased when LBA was incorporated. The Δ*H*m values decreased in all formulations with LBA addition, markedly from 56.7 to 5.97 J/g for PVA15 and PVA15 + LBA, respectively. The rigidity of PCL nanofibers decrease with addition of LBA, as the Young's modulus decreased from about 20 MPa to less than 10 MPa. Excepting for PVA10 nanofibers, the values of elongation at break were similar among control nanofibers and samples with LBA. The nanofibers presented a degree of hemolysis below 2%, so it can be considered as non-hemolytic materials. PVA10 + LBA nanofiber caused no significant toxic effects as evaluated by several models (mutagenicity assay, cell survival measurement, cell viability analysis and agar diffusion cytotoxicity test). In summary, these nanofibers could be used for development of active packaging due to their antimicrobial and antioxidant activities and non-toxic effects.

Acknowledgements Authors thank the Centro de Microscopia e Microanálise (CMM, UFRGS, Brazil) for technical support on electron microscopy and Laboratory of Physical Analysis (ICTA, UFRGS, Brazil) for technical support on thermal and mechanical analyses.

Author contributions AAV: experiments, data analysis, investigation and manuscript writing- original draft preparation; NJC: experiments, data analysis; ALMJ: experiments, data analysis and writing- cytotoxicity potential; FFV: methodology; HCR: methodology and data analysis; AB: writing- review and editing, supervision, and funding. All authors reviewed the final manuscript. All authors have read and agreed to the published version of the manuscript.

Funding This work was supported by Conselho Nacional de Desenvolvimento Científico e Tecnológico (CNPq) [Grant 308880/2021-8 and 405165/2023-4] and Coordenação de Aperfeiçoamento de Pessoal de Nível Superior (CAPES).

Data availability The data that support the findings of this study are available upon reasonable request from the authors.

Declarations

Competing interests The authors declare that they have no known competing financial interests or personal relationships that could have appeared to influence the work reported in this paper.

References

1. Goderska K. The antioxidant and prebiotic properties of lactobionic acid. Appl Microbiol Biotechnol. 2019;103:3737–51.
2. Cardoso T, Marques C, Sotiles AR, Dagostin JLA, Masson ML. Characterization of lactobionic acid evidencing its potential for food industry application. J Food Process Eng. 2019;42: e13277.
3. Sáez-Orviz S, Marcet I, Rendules M, Díaz M. The antimicrobial and bioactive properties of lactobionic acid. J Sci Food Agric. 2022;102:3495–502.
4. Coroli A, Romano R, Saccani A, Raddani N, Mele E, Mascian L. An in-vitro evaluation of the characteristics of zein-based films for the release of lactobionic acid and the effects of oleic acid. Polymers. 2021;13:1826.
5. Cao J, Fu H, Gao L, Zheng Y. Antibacterial activity and mechanism of lactobionic acid against *Staphylococcus aureus*. Folia Microbiol. 2019;64:899–906.
6. Gómez-Estaca J, López-de-Dicastillo C, Hernández-Muñoz P, Catalá R, Gavara R. Advances in antioxidant active food packaging. Trends Food Sci Technol. 2014;35:42–51.
7. Lai WF. Design of polymeric films for antioxidant active food packaging. Int J Mol Sci. 2021;23:12.

8. Yan X, Meng F, Van TT, Wigati LP, Nkede FN, Hamayoon WM, Wardana AA, Tanaka F, Tanaka F. Water barrier coating of chitosan/poly (vinyl alcohol)/trans-cinnamaldehyde regulated postharvest quality and reactive oxygen species metabolism of 'Frutica' tomato (*Solanum lycopersicum* L.). Postharvest Biol Technol. 2024;212:112910.
9. Esmaeilzadeh J, Shabani F, Zak AK. Electrospun poly (ε-caprolactone)/gelatin nanofibrous mats with local delivery of vitamin C for wound healing applications. Colloids Surf A. 2024;687: 133546.
10. Huang X, Du L, Li Z, Yang Z, Xue J, Shi J, Tingting S, Zhai X, Zhang J, Capanoglu E, Zhang N, Sun W, Zou X. *Lactobacillus bulgaricus*-loaded and chia mucilage-rich gum arabic/pullulan nanofiber film: An effective antibacterial film for the preservation of fresh beef. Int J Biol Macromol. 2024;266: 131000.
11. Yang Y, Zheng S, Liu Q, Kong B, Wang H. Fabrication and characterization of cinnamaldehyde loaded polysaccharide composite nanofiber film as potential antimicrobial packaging material. Food Packag Shelf Life. 2020;26: 100600.
12. Priya S, Batra U, Samshritha RN, Sharma S, Charasiya A, Singhvi G. Polysaccharide-based nanofibers for pharmaceutical and biomedical applications: A review. Int J Biol Macromol. 2022;218:209–24.
13. Danagody B, Bose N, Rajappan K. Electrospun polyacrylonitrile-based nanofibrous membrane for various biomedical applications. J Polym Res. 2024;31:119.
14. Veras FF, Ritter AC, Roggia I, Pranke P, Pereira CN, Brandelli A. Natamycin-loaded electrospun poly(ε-caprolactone) nanofibers as an innovative platform for antifungal applications. SN Appl Sci. 2020;2:1105.
15. Parın FN, Ullah A, Yeşilyurt A, Parın U, Haider MK, Kharaghani D. Development of PVA-psyllium husk meshes via emulsion electrospinning: preparation, characterization, and antibacterial activity. Polymers. 2022;14:1490.
16. Parin FN, Terzioğlu P, Sicak Y, Yildirim K, Öztürk M. Pine honey-loaded electrospun poly (vinyl alcohol)/gelatin nanofibers with antioxidant properties. J Text Inst. 2021;112:628–35.
17. Yavari Maroufi L, PourvatanDoust S, Naeijian F, Ghorbani M. Fabrication of electrospun polycaprolactone/casein nanofibers containing green tea essential oils: applicable for active food packaging. Food Bioprocess Technol. 2022;15:2601–15.
18. Re R, Pellegrini N, Proteggente A, Pannala A, Yang M, Rice-Evans C. Antioxidant activity applying an improved ABTS radical cation decolorization assay. Free Radiat Biol Med. 1999;26:1231–7.
19. Mosayebi V, Fathi M, Shahedi M, Soltanizadeh N, Emam-Djomeh Z. Fast-dissolving antioxidant nanofibers based on Spirulina protein concentrate and gelatin developed using needleless electrospinning. Food Biosci. 2022;47: 101759.
20. Canbolat MF, Celebioglu A, Uyara T. Drug delivery system based on cyclodextrin-naproxen inclusion complex incorporated in electrospun polycaprolactone nanofibers. Colloids Surf B. 2014;115:15–21.
21. ASTM. Standard Test Method for Tensile Properties of Plastics. American Society for Testing and Materials. 2014, D 638-14.
22. Mortelmans K, Zeiger E. The Ames *Salmonella*/microsome mutagenicity assay. Mutat Res. 2000;455:29–60.
23. ISO 10993-5:2009. Biological evaluation of medical devices - Part 5: Tests for in vitro cytotoxicity. International Organization for Standardization. 2009.
24. Franken NA, Rodermond HM, Stap J, Haveman J, Van Bree C. Clonogenic assay of cells in vitro. Nat Protoc. 2006;1:2315–9.
25. Mosmann T. Rapid colorimetric assay for cellular growth and survival: application to proliferation and cytotoxicity assays. J Immunol Methods. 1983;65:55–63.
26. Lehmann DM, Richardson ME. Impact of assay selection and study design on the outcome of cytotoxicity testing of medical devices: the case of multi-purpose vision care solutions. Toxicol In Vitro. 2010;24:1306–13.
27. Malikmannadov E, Tanir TE, Kiziltay A, Hasirci V, Hasirci N. PCL and PCL-based materials in biomedical applications. J Biomater Sci Polym Ed. 2018;29:863–93.
28. Isaia HA, Pinilla CMB, Brandelli A. Evidence that protein corona reduces the release of antimicrobial peptides from polymeric nanocapsules in milk. Food Res Int. 2021;140: 110074.
29. Abd El-Mohdy HL, Aly HM. Characterization, properties and antimicrobial activity of radiation induced phosphorus-containing PVA hydrogels. Arab J Sci Eng. 2023;48:341–51.
30. Kusumawati DH, Munasir, Rohmawati L, Uzalia P, Layli MD, Rahanti AB, Yuliani I. Effectiveness of polyvinyl alcohol nanofiber composites as anti-bacterial materials in wound dressing. J Phys Conf Ser. 2022;2392:012018.
31. Chuysinuan P, Thanyacharoen T, Techasakul S, et al. Electrospun characteristics of gallic acid-loaded poly vinyl alcohol fibers: Release characteristics and antioxidant properties. J Sci Adv Mater Devices. 2018;3:175–80.
32. Uebel LS, Schmatz DA, Kuntzler SG, Dora CL, Muccillo-Baisch AL, Costa JAV, De Morais MG. Quercetin and curcumin in nanofibers of polycaprolactone and poly(hydroxybutyrate-co-hydroxyvalerate): assessment of in vitro antioxidant activity. J Appl Polym Sci. 2016;133:app.43712.
33. Zhang Z, Su W, Li Y, Zhang S, Liang H, Ji C, Lin X. High-speed electrospinning of phycocyanin and probiotics complex nanofibrous with higher probiotic activity and antioxidation. Food Res Int. 2023;167: 112715.
34. Apak R, Özyürek M, Güçlü K, Çapanoğlu E. Antioxidant activity/capacity measurement. 1. Classification, physicochemical principles, mechanisms, and electron transfer (ET)-based assays. J Agric Food Chem. 2016;64:997–1027.
35. Oudjedi K, Manso S, Nerin C, Hassissen N, Zaidi F. New active antioxidant multilayer food packaging films containing Algerian Sage and Bay leaves extracts and their application for oxidative stability of fried potatoes. Food Control. 2019;98:216–26.
36. Zehetmeyer G, Meria SMM, Scheibel JM, Silva CB, Rodembusch FS, Brandelli A, Soares RMD. Biodegradable and antimicrobial films based on poly(butylene adipate-co-terephthalate) electrospun fibers. Polym Bull. 2017;74:3243–68.
37. Qiu H, Zhu S, Pang L, Ma J, Liu Y, Du L, Wu Y, Jin Y. ICG-loaded photodynamic chitosan/polyvinyl alcohol composite nanofibers: Anti-resistant bacterial effect and improved healing of infected wounds. Int J Pharm. 2020;588: 119797.
38. Gonçalves RP, Silva FFF, Picciani PHS, Dias ML. Morphology and thermal properties of core-shell PVA/PLA ultrafine fibers produced by coaxial electrospinning. Mater Sci Appl. 2015;6:189–99.
39. Mollaghadimi B. Preparation and characterization of polycaprolactone-fibroin nanofibrous scaffolds containing allicin. IET Nanobiotechnol. 2022;16:239–49.

40. Xu L, Park JA, Kattel K, Bony BA, Heo WC, Jim S, Park JW, Chang Y, Do JY, Chae KS, Kim TJ, Park JA, Kwak YW, Lee GH. A T1, T2 magnetic resonance imaging (MRI)-fluorescent imaging (FI) by using ultrasmall mixed gadolinium-europium oxide nanoparticles. New J Chem. 2012;36:2361–7.
41. Veras FF, Roggia I, Pranke P, Pereira CN, Brandelli A. Inhibition of filamentous fungi by ketoconazole-functionalized electrospun nanofibers. Eur J Pharm Sci. 2016;84:70–6.
42. Alavarse AC, Silva FWO, Colque JT, Silva VM, Prieto T, Venancio EC, Bonvent JJ. Tetracycline hydrochloride-loaded electrospun nanofibers mats based on PVA and chitosan for wound dressing. Mater Sci Eng C. 2017;77:271–81.
43. Katančić Z, Travaš-Sejdić J, Hrnjak-Murgić ZZ. Study of flammability and thermal properties of high-impact polystyrene nanocomposites. Polym Degrad Stab. 2011;96:2104–11.
44. Ippel BD, Van Haaften EE, Bouten CVC, Dankers PYW. Impact of additives on mechanical properties of supramolecular electrospun scaffolds. ACS Appl Polym Mater. 2020;2:3742–8.
45. DeFelice J, Lipson JEG. The influence of additives on polymer matrix mobility and the glass transition. Soft Matter. 2021;17:376–87.
46. Szlachetka O, Witkowska-Dobrev J, Baryła A, Dohojda M. Low-density polyethylene (LDPE) building films—tensile properties and surface morphology. J Build Eng. 2021;44: 103386.
47. Handayani SU, Fahrudin M, Mangestiyono W, Hadi Muhamad AF. Mechanical properties of commercial recycled polypropylene from plastic waste. J Vocat Stud Appl Res. 2021;3:1–4.
48. Brandelli A. Nanocomposites and their applications in antimicrobial packaging. Front Chem. 2024;12:1356304.
49. Nguyen SV, Lee BK. Multifunctional nanocomposite based on polyvinyl alcohol, cellulose nanocrystals, titanium dioxide, and apple peel extract for food packaging. Int J Biol Macromol. 2023;227:551–63.
50. Sæbø IP, Bjørås M, Franzyk H, Helgesen E, Booth JA. Optimization of the hemolysis assay for the assessment of cytotoxicity. Int J Mol Sci. 2023;24:2914.
51. Ekambaram R, Saravanan S, Babu VPS, Dharmalingam S. Fabrication and evaluation of Docetaxel doped ZnO nanoparticles incorporated PCL nanofibers for its hemocompatibility, cytotoxicity andapoptotic effects against A549. Materialia. 2022;21: 101278.
52. ASTM F756-17. Standard Practice for Assessment of Hemolytic Properties of Materials. American Standard for Testing Materials. Annual Book of ASTM Standards Volume: 13.01, USA, 2017.
53. Kohl Y, Rundén-Pran E, Mariussen E, Hesler M, El Yamani N, Longhin EM, Dusinska M. Genotoxicity of nanomaterials: Advanced in vitro models and high throughput methods for human hazard assessment—a review. Nanomaterials. 2020;10:1911.
54. Ren N, Atyah M, Chen WY, Zhou CH. The various aspects of genetic and epigenetic toxicology: testing methods and clinical applications. J Transl Med. 2017;15:110.
55. Perry KL, Walker GG. Identification of plasmid (pKM101)-coded proteins involved in mutagenesis and UV resistance. Nature. 1982;300:278–81.
56. Tani N, Kinoshita S, Okamoto Y, Kotani M, Itagaki H, Murakami N, Sugiura S, Usami M, Kato K, Kojima H, Ohno T, Saijo K, Kato M, Hayashi M, Ohno Y. Interlaboratory validation of the in vitro eye irritation tests for cosmetic ingredients. (8) Evaluation of cytotoxicity tests on SIRC cells. Toxicol In Vitro. 1999;13:175–87.
57. Lee H, Park K. In vitro cytotoxicity of zinc oxide nanoparticles in cultured statens seruminstitut rabbit cornea cells. Toxicol Res. 2019;35:287–94.
58. Borefreund E, Babich H, Martin-Alguacil N. Comparisons of two in vitro cytotoxicity assays—the neutral red (NR) and tetrazolium MTT tests. Toxicol In Vitro. 1988;2:1–6.
59. Parin FN, Ullah S, Yildrim K, Hashmi M, Kim I-S. Fabrication and characterization of electrospun folic acid/hybrid fibers: In vitro controlled release study and cytocompatibility assays. Polymers. 2021;13:3594.
60. Ghasemi M, Turnbull T, Sebastian S, Kempson I. The MTT assay: Utility, limitations, pitfalls, and interpretation in bulk and single-cell analysis. Int J Mol Sci. 2021;22:12827.
61. Oldham RK, Siwarski D, McCoy JL, Plata EJ, Herberman RB. Evaluation of a cell-mediated cytotoxicity assay utilizing 125 iododeoxyuridine-labeled tissue-culture target cells. Natl Cancer Inst Monogr. 1973;37:49–58.
62. Uhljar LE, Ambrus R. Electrospinning of potential medical devices (wound dressings, tissue engineering scaffolds, face masks) and their regulatory approach. Pharmaceutics. 2023;15:417.